Performance Assessment of UD-NCF CFRP Double-Hat Channels under Oblique Crush Loading

Ningwei Huang[1*], John Montesano[1]

[1] Composites Research Group, Department of Mechanical & Mechatronics Engineering, University of Waterloo, 200 University Ave, Waterloo, Ontario, Canada, N2L 3G1

* *Corresponding author (ningwei.huang@uwaterloo.ca)*

Keywords: *CFRP composites; Oblique impact; Energy absorption; Finite element analysis*

1. Abstract

Vehicle frontal crush structures must be designed to effectively absorb energy under both axial and ±30° oblique impact conditions to meet automotive crashworthiness requirements. Owing to their excellent energy absorption characteristics, carbon fiber-reinforced plastic (CFRP) composites have emerged as candidate materials for such applications. This study investigates the energy absorption characteristics of adhesively bonded unidirectional non-crimp carbon fabric (UD-NCF) CFRP double-hat channels under oblique crush loading. Channels with $[0/\pm45/90]_s$ and $[\pm45/0_2]_s$ stacking sequences were tested under 30° off-axis quasi-static compressive loading. Stable and progressive channel crushing was observed in channels with both stacking sequences, where lamina bending was identified as the dominant failure mode. A structural simulation model was developed using an explicit finite element solver where a damage-based material model was employed to capture the failure behavior of the UD-NCF composite material. The numerical predictions were validated against experimental results with reasonable accuracy, which will enable use of the developed simulation model for future frontal crush structure design.

2. Introduction

In recent years, carbon fiber-reinforced plastic (CFRP) composite materials have emerged as a promising lightweight solution for vehicle structures due to their exceptional specific strength and stiffness, excellent energy absorption characteristics, high design flexibility and low maintenance cost [1]. Although their application in the automotive industry was previously limited by high material and manufacturing costs and long production cycle times [2], recent technological advancements in automated liquid composite molding processes such as high-pressure resin transfer molding (HP-RTM), development of new rapid-curing resin systems, and relatively low-cost heavy-tow unidirectional non-crimp carbon fabrics (UD-NCFs), have siginificantly reduced the production cycle times from hours to minutes [3].

From a crashworthiness perspective, vehicle structures must effectively absorb energy under various impact conditions to ensure occupant protection and, thus, meet safety requirements. To incorportate high performance CFRP composites into vehicle structures, it is essential to understand their complex energy absorbing behaviours due to their anisotropic response and heterogeneous nature. Multiple damage mechanisms, including fiber rupture, fiber kinking, matrix cracking and delamination, can occur simultaneously, making it quite challenging to determine whether observed failures are caused by a single mode or a combination of interacting mechanisms [4-6].

Despite the advantages of CFRP composites, previous studies have primarily focused on unidirectional tape or woven fabric CFRP structures [7-9] with comparatively few studies evaluating the crush performance and energy absorption capacity of UD-NCF CFRP components. Recently, Harvey et al. [10] studied the dynamic axial crush performance of UD-NCF carbon fiber/epoxy composite channels with hat and corrugated cross-sectional geometries. Two stacking sequences were considered, namely $[0/\pm45/90]_s$ and $[\pm45/0_2]_s$, where channels with the latter sequence exhibited higher overall energy absorption owing to a greater number of plies aligned with the loading axis. Similar observations were reported by Ajayi [11], who investigated UD-NCF CFRP tapered hat channels with stacking sequences $[0/\pm45/90]_s$, $[0/90/\pm45]_s$ and $[\pm45/0_2]_s$ under dynamic axial compressive loading.

Furthermore, only a limited number of studies have investigated the effects of oblique loading on the crush performance of composite structures, and they are mainly restricted to closed-profile tubes [12-14]. No research to date has assessed the crush performance of UD-NCF composite components under oblique loading conditions.

Therefore, this study aims to investigate the energy absorption characteristics of adhesively bonded UD-NCF CFRP double-hat channels under oblique crush loading using both experiments and computational simulations.

3. Quasi-static oblique crushing experiments

3.1. Materials and specimen preparation

The material system consisted of a carbon fiber fabric and a snap-cure epoxy resin system. The reinforcement was a 50K stitch-bonded unidirectional non-crimp fabric, namely PX35-UD300 (Zoltek™). The matrix comprised a three-part resin system, including a fast-cure epoxy resin EPIKOTE™ Resin TRAC 06150, a hardener EPIKURE™ Curing Agent TRAC 06150, and an internal mold release agent HELOXY™ Additive TRAC 06805 (Westlake Epoxy). Hat channel parts measuring 800 mm in length were fabricated using a High-Pressure Resin Transfer Molding (HP-RTM) process. The cross-sectional geometry of the hat channels is shown in Figure 1(a). Double hat channel specimens were fabricated by adhesively bonding two trimmed 190 mm long hat channel parts following the bonding procedure reported by Ajayi [11]. Two hat channels were bonded together using an impact-resistant structural adhesive (3M™ 07333) with a bond-line thickness of 0.65mm. The bonded specimens were then trimmed to an overall length of approximately 153 mm, and a 45-degree chamfer (2.5-3 mm) was machined on one end of specimens to serve as a progressive crush trigger (Figure 1(b)). Two stacking sequences, $[0/\pm45/90]_s$ and $[\pm45/0_2]_s$, were considered with an average laminate thickness of 2.72 mm.

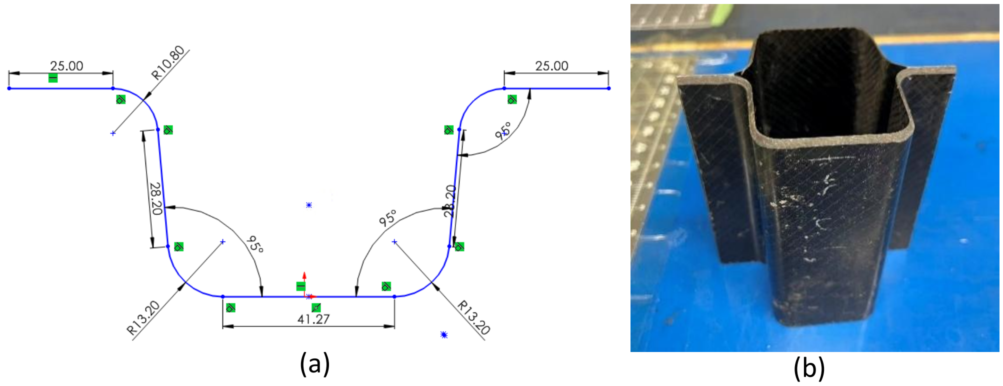

Figure 1. Cross-sectional geometry of single hat channels (a) and fabricated double hat channels with a 45-degree chamfer machined on one end of the channel (b).

3.2. *Experimental setup for quasi-static oblique crush tests*

Quasi-static oblique crush tests were conducted on double hat channel specimens using a 120-ton Macrodyne hydraulic press (Figure 2). The load was measured using three Tovey SW20-50kip load cells, each with a capacity of 50,000 lb, mounted behind the upper impactor plate. Tests were performed under displacement control with a constant velocity of 1 mm/s to ensure quasi-static loading conditions. Crushing was prescribed over a displacement of approximately 80 mm. The displacement data were captured via feedback provided by a PID-controlled motion system.

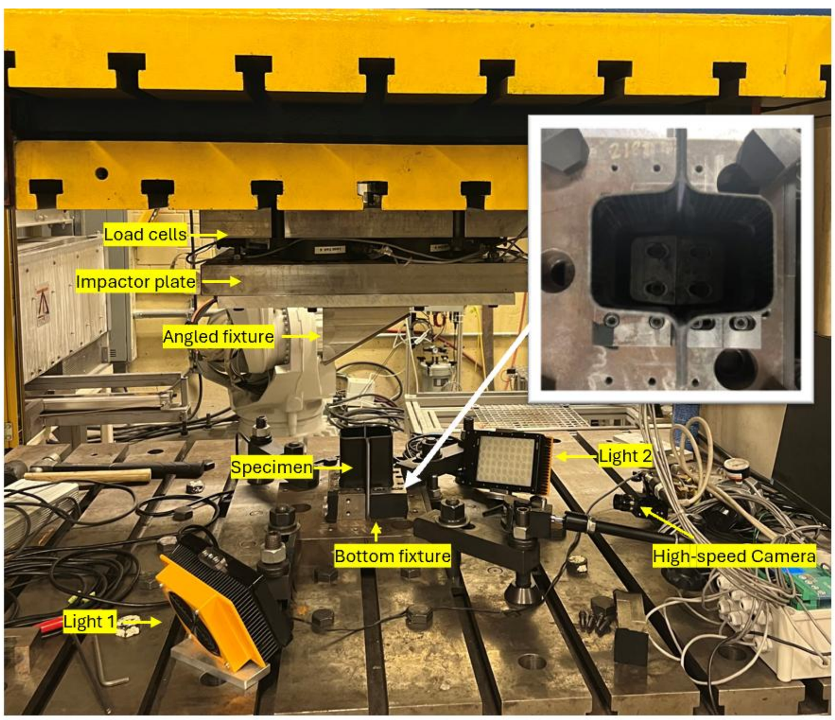

Figure 2. Experimental setup of quasi-static oblique loading tests.

Two steel mounting fixtures, originally designed by Ajayi [11], were used to constrain the bottom end of the specimens to a custom-designed raised lower platform. A new angled fixture was mounted on the upper impactor plate to impose the prescribed 30° oblique loading condition

(Figure 3). The crushing process was captured by two high-speed Photron SA-Zs cameras with one positioned at the side of the specimen and the other mounted on a tripod oriented in front of the specimen. Both cameras captured images at a frame rate of eight frames per second. Two external lighting units were positioned laterally to provide appropriate illumination of the specimen throughout the test, avoiding underexposure or overexposure.

For each stacking sequence, three quasi-static oblique tests were conducted to ensure repeatability. Crush force–displacement data were acquired at a sampling frequency of 200 Hz with a cutoff frequency of 5 Hz. The mass per unit length of the double-hat channel specimens was measured to be approximately 1.83 g/mm.

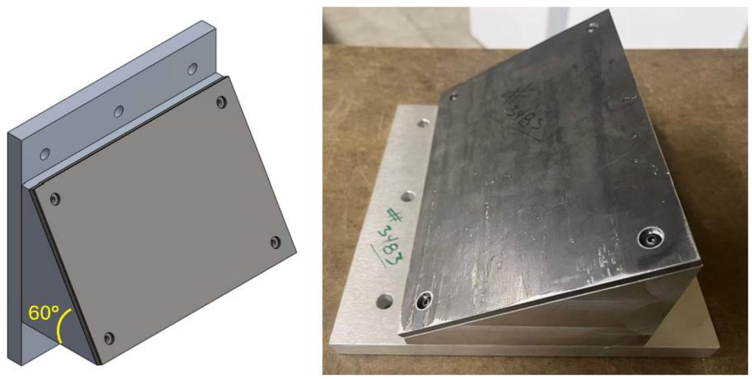

(a) (b)

Figure 3. CAD model of the angled fixture developed in SolidWorks (a) and the corresponding manufactured fixture (b).

3.3. Experimental results

The force–displacement responses and specific energy absorption for double hat channel specimens with $[0/\pm45/90]_s$ and $[\pm45/0_2]_s$ stacking sequences under quasi-static oblique loading are presented in Figures 4 and 5, respectively. Table 1 summarizes the average total energy absorption (EA) and SEA for each stacking sequence.

The double hat channel specimens with both stacking sequences exhibited stable and progressive crushing for the duration of the performed tests. Lamina bending was observed as the primary failure mode for the channel flanges and upper walls, while the channel side walls failed in a more brittle manner. In comparison, the double hat channel specimens comprising the stiffer $[\pm45/0_2]_s$ stacking sequence (i.e., four 0° layers oriented along the loading axis) achieved a 6.4% higher total energy absorption and a 9.95% higher SEA when compared to the specimens comprising the more compliant quasi-isotropic $[0/\pm45/90]_s$ stacking sequence. However, the enhanced axial stiffness of the $[\pm45/0_2]_s$ laminate also increased susceptibility to localized compressive instability, leading to fiber kinking and brittle fracture under oblique loading (Figure 7). In contrast, double hat channels with the $[0/\pm45/90]_s$ stacking sequence exhibited a greater tendency toward brittle fracture accompanied by matrix cracking, which was less pronounced in the $[\pm45/0_2]_s$ configuration (Figure 6).

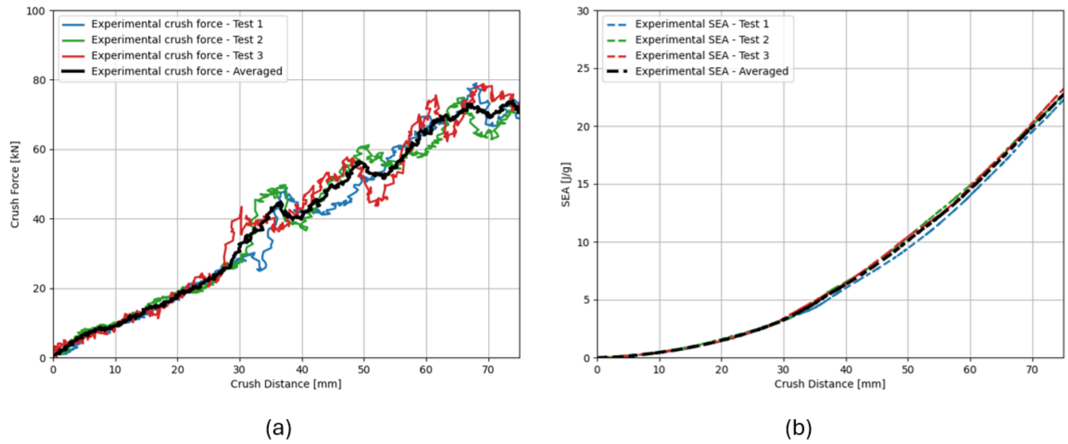

Figure 4. Crush force-displacement response (a) and SEA (b) for $[0/\pm45/90]_s$ double hat channel specimens.

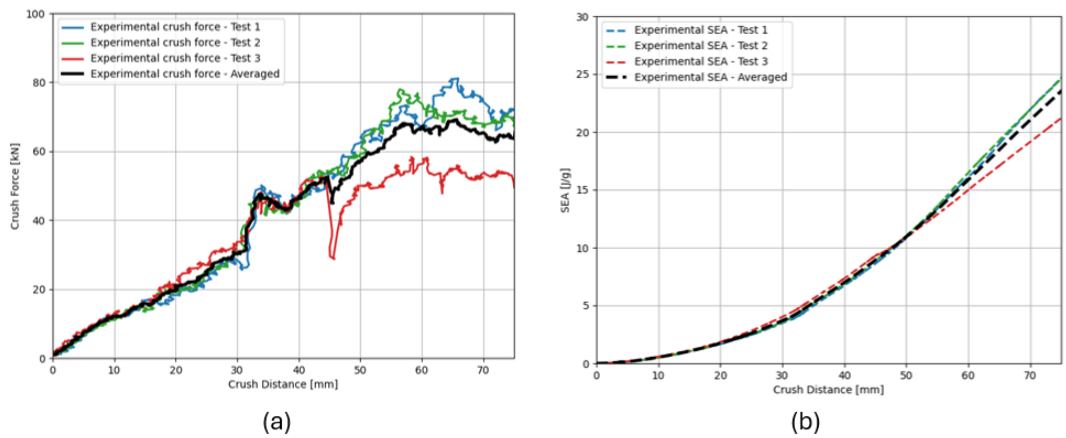

Figure 5. Crush force-displacement response (a) and SEA (b) for $[\pm45/0_2]_s$ double hat channel specimens.

Table 1. Average total energy absorption and SEA computed up to displacement at peak force for double channel specimens tested under quasi-static oblique crushing.

Geometry	Crush Displacement Used [mm]	Crushed Mass [g]	EA [J]	SEA [J/g]
$[0/\pm45/90]_s$ Double hat channel	68	117.73	2371.8	20.1
$[\pm45/0_2]_s$ Double hat channel	66	114.19	2523.8	22.1

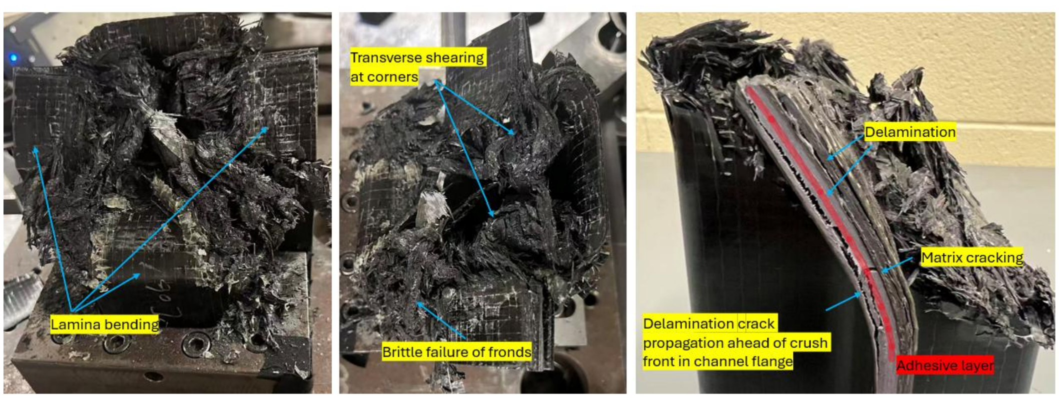

Figure 6. Post-crush images for $[0/\pm45/90]_s$ double hat channel specimen under quasi-static oblique crush loading.

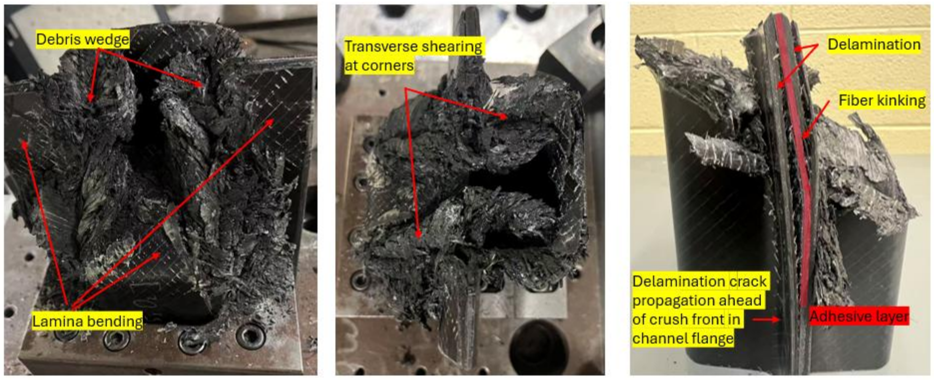

Figure 7. Post-crush images for $[\pm 45/0_2]_s$ double hat channel specimens under quasi-static oblique crush loading.

4. Quasi-static oblique simulation model

4.1. LS-DYNA simulation model description

A structural simulation model was developed to simulate the performed oblique crush tests using the explicit time-integration finite element software LS-DYNA. The double hat channel specimen was modelled using two identical hat channels and two flat strips positioned centrally within the gap between each pair of flanges, representing the adhesive layers (Figure 8). The mid-plane surface of each hat channel was meshed using structured quadrilateral shell elements in HyperMesh software, with an element size of 5 mm. All elements were defined as fully integrated BELYTSCHKO-TSAY shell elements (Type 16), with a ply thickness of 0.34 mm. The Type 16 shell formulation was selected to ensure sufficient accuracy with minimum computational cost. Hourglass control was applied to both the channel and trigger regions (IHG = 8) to introduce warping stiffness and improve numerical stability and solution convergence. The crush triggers with a length of 3 mm were modelled at the impacted end of the double hat channel using structured quadrilateral elements with a size of 3 mm. The trigger elements were assigned a reduced shell thickness, equal to half of the channel thickness (0.17 mm per ply).

The rigid impactor wall was meshed with 10 mm structured quadrilateral shell elements and was also defined using Type 16 fully integrated shell elements with a thickness of 0.5 mm. Mass elements were assigned to each node of the impactor wall to achieve a total mass of 100 kg, representing the upper plate used in the hydraulic press for the quasi-static oblique experiments. As shown in Figure 8(a), the impactor wall was oriented 30-degree relative to the global Y-axis to model the off-axis loading condition.

The adhesive layers (Figure 8(b)) were modelled using 8-node solid cohesive elements with four through-thickness integration points (ELFORM = 20). Based on the mesh sensitivity study reported by Ajayi [11], a cohesive element size of 0.65 mm × 1 mm × 1 mm was adopted in the model, as such mesh size was shown to be sufficient to reproduce the experimentally observed adhesive bonding behaviour.

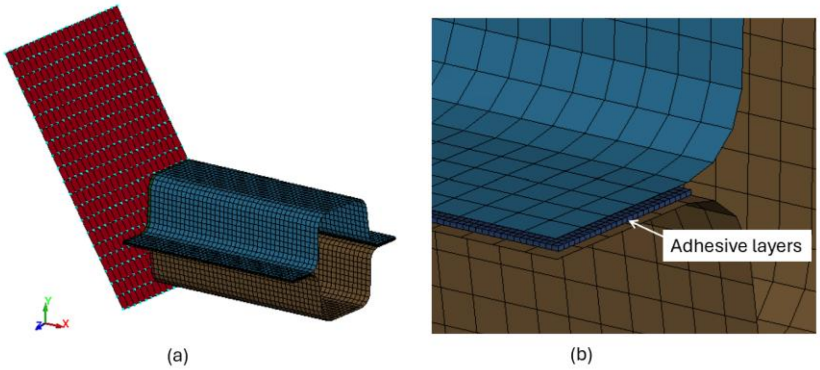

Figure 8. LS-DYNA model of double hat channel (a) and adhesive layers (b).

In addition, a single-shell modeling approach was adopted to achieve computational and time efficiency. The *PART_COMPOSITE card was employed to define the ply orientations of the laminated composite channel and the crush trigger region. For each ply, one integration point was assigned with the corresponding material direction and mechanical properties. Adhesive bonding between each pair of double hat channel flanges and adhesive layers was represented using the *CONTACT_TIED_SHELL_EDGE_TO_SURFACE formulation.

For the boundary and loading conditions, a length of 50 mm at the bottom of the channel was constrained in six degrees of freedom to represent the mounting fixtures used to fix one end of the channel during the experiments. Under quasi-static crushing, the impactor wall was defined using a prescribed constant displacement rate of 90 mm/s, where the impact velocity was scaled up from 1mm/s to reduce the computational time. The *CONTACT_AUTOMATIC_SINGLE_SURFACE card was employed to model contact interactions, with static and dynamic friction coefficients set to 0.2. Reaction forces between the impactor and the structure were extracted using the *CONTACT_FORCE_TRANSDUCER_PENALTY card. The simulation termination time was set to 1 s.

The UD-NCF composite channels and their corresponding crush triggers were modeled with the material model MAT_054 (*MAT_ENHANCED_COMPOSITE_DAMAGE). The required mechanical properties were obtained from experimental studies reported by Rouf et al. [2] and Suratkar [15], including a strength–strain rate relationship to account for the strain-rate sensitivity of the UD-NCF composite material. Additionally, the initial values of non-physical parameters were selected based on the recommendations reported by Ajayi [11] while DFAILC (compressive failure strain in fiber direction) and DT (strain rate averaging option) were recalibrated as -0.4 and 1, respectively. The structural adhesive was modeled using MAT_240 (*MAT_COHESIVE_MIXED_MODE_ELASTOPLASTIC_RATE) with input parameters adopted from Watson [16] for the same adhesive.

4.2. Simulation results and model validation

The predicted force-displacement response and SEA for double hat channel specimens with both stacking sequences were compared with experimental results (Figures 9 and 10) and a quantitative comparison is summarized in Table 2. The simulated results were processed using a SAE filter with a frequency of 5 Hz.

Under quasi-static oblique loading, the model with specimen comprising a $[0/\pm45/90]_s$ stacking sequence accurately captured the initial slope of the force-displacement response up to approximately 37 mm crush displacement, corresponding to the onset of local flange bending. The predicted results beyond this point were not included because the simulation was terminated due to excessive computational time and cost associated with severe cohesive element distortion and a continuously decreasing time step. In contrast, for the $[\pm45/0_2]_s$ stacking sequence, the model captured the entire crushing response, although both peak and post-peak forces were underpredicted. Overall, the SEA values were underestimated by 16% and 24% for $[0/\pm45/90]_s$ and $[\pm45/0_2]_s$ configurations, respectively. These discrepancies may be attributed to modelling limitations, including the exclusion of clamping pressure on the mounting fixture and the inability of MAT_054 material model to capture interlaminar damage. Additionally, the differences in stacking sequence lead to distinct failure mechanisms: the $[0/\pm45/90]_s$ laminate exhibits more brittle behavior, accelerating cohesive element distortion and unphysical deformation, whereas the $[\pm45/0_2]_s$ laminate promotes more stable, shear-dominated progressive crushing.

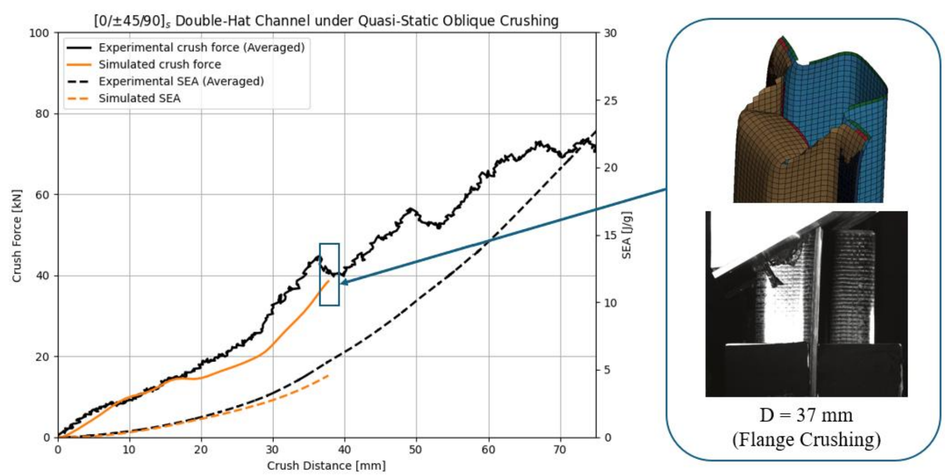

Figure 9. Predicted results for $[0/\pm45/90]_s$ double hat channel under quasi-static oblique crushing.

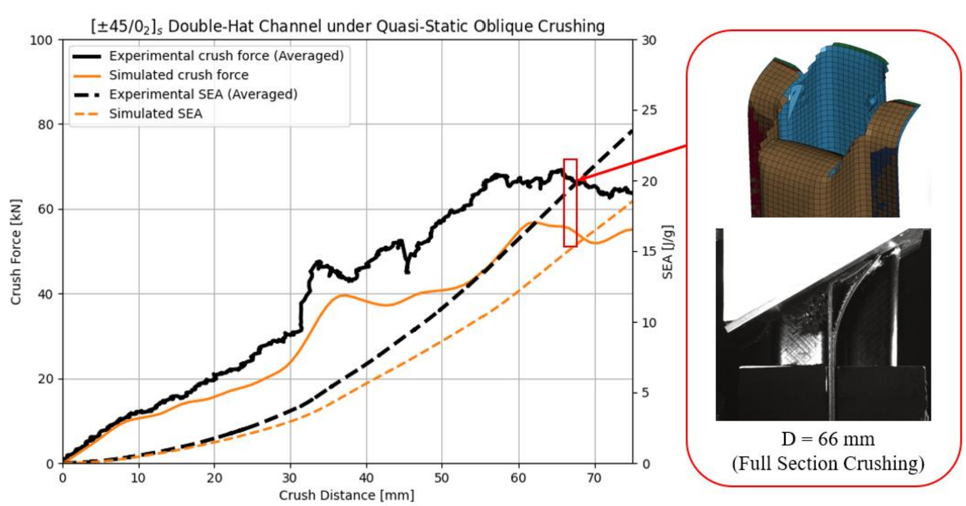

Figure 10. Predicted results for $[\pm45/0_2]_s$ double hat channel under quasi-static oblique crushing.

Table 2. Quantitative comparison between predicted and average experimental SEA values.

Geometry	Predicted SEA [J/g]	Experimental SEA [J/g]	%Error
$[0/\pm45/90]_s$ Double hat channel	4.3 +	5.0	16
$[\pm45/0_2]_s$ Double hat channel	16.7 *	22.1	24

* Results captured up to the peak force.
\+ Results captured up to computational model termination.

5. Conclusion

Experimentally, the double hat channels with both $[0/\pm45/90]_s$ and $[\pm45/0_2]_s$ stacking sequences exhibited stable and progressive crushing under quasi-static oblique loading, with lamina bending as dominant failure mode. The $[\pm45/0_2]_s$ configuration demonstrated superior energy absorption, achieving 6.4% higher total energy absorption and 9.95% higher specific energy absorption compared to the $[0/\pm45/90]_s$ laminate. The developed simulation model captured the initial response of the $[0/\pm45/90]_s$ laminate but terminated prematurely due to excessive computational time and cost, while the model predicted the full crushing process of the $[\pm45/0_2]_s$ laminate with underpredicted SEA by 24%. Future numerical work will focus on further calibration of the employed material model as well as developing a multi-layer shell simulation model to capture delamination.

6. References

[1] C. W. Isaac and C. Ezekwem, "A review of the crashworthiness performance of energy absorbing composite structure within the context of materials, manufacturing and maintenance for sustainability," Composite Structures, vol. 257, p. 113081, Feb. 2021, doi: 10.1016/j.compstruct.2020.113081.

[2] K. Rouf, “Characterizing and Modelling the Strain Rate-Dependent Constitutive Response of a Unidirectional Non-Crimp Fabric Composite Material,” PhD Thesis, University of Waterloo, Waterloo, Canada, 2023.

[3] A. Cherniaev, Y. Zeng, D. Cronin, and J. Montesano, "Quasi-static and dynamic characterization of unidirectional non-crimp carbon fiber fabric composites processed by HP-RTM," *Polymer Testing*, vol. 76, pp. 365-375, Jul. 2019, doi: 10.1016/j.polymertesting.2019.03.036.

[4] G. Lu and T. Yu, " Composite materials and structures," in *Energy Absorption of Structures and Materials*, Woodhead Publishing Series in Metals and Surface Engineering, 2003, pp. 317-350.

[5] A. G. Mamalis, M. Robinson, G. A. Demosthenous, M. B. Ioannidis, J. Carruthers, and D. E. Manolakos, "Crashworthy capability of composite material structures," *Compos. Struct.*, vol. 37, no. 2, pp. 109-134, 1997, doi: 10.1016/S0263-8223(97)80005-0.

[6] W. C. Hwang, C. S. Cha, and I. Y. Yang, "Optimal crashworthiness design of CFRP hat shaped section member under axial impact," *Mater. Res. Innov.,* vol. 15, no. 1, pp. 324-327, 2011, doi: 10.1179/143307511X12858957674472.

[7] X. Zhao, G. Zhu, C. Zhou, and Q. Yu, "Crashworthiness analysis and design of composite tapered tubes under multiple load cases," *Compos. Struct.,* vol. 222, p. 110920, 2019, doi: 10.1016/j.compstruct.2019.110920.

[8] D. Hu, Y. Wang, L. Dang, and Q. Pan, "Energy absorption characteristics of composite tubes with different fibers and matrix under axial quasi-static and impact crushing conditions," *J. Mech. Sci. Technol.*, vol. 32, no. 6, pp. 2587–2599, Jun. 2018, doi: 10.1007/s12206-018-0516-y.

[9] G. Sun, S. Li, G. Li, and Q. Li, "On crashing behaviors of aluminum/CFRP tubes subjected to axial and oblique loading: An experimental study," *Compos. Part B Eng.*, vol. 145, pp. 47–56, Jul. 2018, doi: 10.1016/j.compositesb.2018.02.001.

[10] B. Harvey, "Characterization of the axial crush and bending response of carbon fiber non-crimp fabric/snap-cure epoxy under different loading rates," University of Waterloo, Waterloo, Canada, Internal Report (Composites Research Group), 2022.

[11] V. Ajayi, "Experimental Characterization and Numerical Modelling of the Energy Absorption Capacity of UD-NCF Carbon Fibre/Epoxy Composite Channels," MASc thesis, Waterloo, Canada, 2025.

[12] H. Ghasemnejad and H. Hadavinia, "Off-axis crashworthiness characteristic of woven glass/epoxy composite box structures," *Journal of Reinforced Plastics and Composites*, vol. 29, no. 15, pp. 2306–2330, Aug. 2010, doi: 10.1177/0731684409347807.

[13] A. Rabiee and H. Ghasemnejad, "Laminate tailoring of composite tubular structures to improve crashworthiness design at off-axis loading," *Open Journal of Composite Materials*, vol. 8, pp. 84–109, Jul. 2018, doi: 10.4236/ojcm.2018.83008.

[14] H. Song and X. Du, "Off-axis crushing of GFRP tubes," *Composites Science and Technology*, vol. 62, no. 15, pp. 2065–2073, Nov. 2002, doi: 10.1016/S0266-3538(02)00152-5.

[15] A. P. Suratkar, "Damage in non-crimp fabric carbon fiber reinforced epoxy composites under various mechanical loading conditions", Ph.D. thesis, Univ. of Western Ontario, London, ON, Canada, 2022.

[16] B. Watson, M. J. Worswick, and D. S. Cronin, "Quantification of mixed mode loading and bond line thickness on adhesive joint strength using novel test specimen geometry," *Int. J. Adhes.,* vol. 102, p. 102682, 2020, doi: 10.1016/j.ijadhadh.2020.102682.